Short Communication:

Synthesis, Characterization, and Magnetic Properties of Iron(II) Complex with 2,6-Bis(pyrazol-3-yl)pyridine Ligand and Tetracyanonickelate Anion

Fitriani Fitriani[1], Irma Mulyani[1*], Djulia Onggo[1], Kristian Handoyo Sugiyarto[2], Ashis Bhattacharjee[3], Hiroki Akutsu[4], and Anas Santria[4,5]

[1]*Inorganic and Physical Chemistry Research Group, Faculty of Mathematics and Natural Sciences, Institut Teknologi Bandung, Jl. Ganesha 10, Bandung 40132, Indonesia*

[2]*Department of Chemistry Education, Universitas Negeri Yogyakarta, Jl. Colombo No. 1, Yogyakarta 55281, Indonesia*

[3]*Department of Physics, Visva-Bharati University, Santiniketan 731204, India*

[4]*Graduate School of Science, Osaka University, 1-1 Machikaneyama, Toyonaka, Osaka 560-0043, Japan*

[5]*Research Center for Chemistry, National Research and Innovation Agency, Kawasan PUSPITEK, Serpong, Tangerang Selatan, Banten 15314, Indonesia*

**** Corresponding author:***

email: imulyani@itb.ac.id

Received: January 24, 2023
Accepted: March 3, 2023

DOI: 10.22146/ijc.81625

Abstract: *The complex containing iron(II), 2,6-bis(pyrazol-3-yl)pyridine (3-bpp) as ligand, and tetracyanonickelate as counter anion has been synthesized and characterized. The characterization data suggest the corresponding formula of* $[Fe(3\text{-}bpp)_2][Ni(CN)_4]\cdot 4H_2O$*. Meanwhile, the SEM–EDX analysis image confirms the existence of all elements contained in the complex except the hydrogen atom. The infrared spectra exhibit vibration bands of the functional groups of 3-bpp ligand and* $[Ni(CN)_4]^{-1}$ *anion. From magnetic property measurement, the complex's molar magnetic susceptibility* (X_MT) *value is 2.65 emu mol*$^{-1}$ *K at 300 K, which contains about 75% high-spin state of the Fe(II) complex. Upon lowering the temperature, the* X_MT *value gradually decreases around 1.37 emu mol*$^{-1}$ *K at 13 K. It decreases sharply to about 0.73 emu mol*$^{-1}$ *K at 2 K. These values reveal that Fe(II) complex is in the low-spin (LS) state. As a result, the complex exhibited spin-crossover characteristics of gradual transition without thermal hysteresis, and the transition temperature occurred below room temperature with a transition temperature* ($T_{1/2}$) *close to 140 K. The spin crossover property of the complex is supported by a thermochromic reversible color change from red-brown at room temperature to dark brown on cooling in liquid nitrogen associated with the high-spin to low-spin transition.*

Keywords: *iron(II); spin crossover; tetracyanonickelate; 2,6-bis(pyrazol-3-yl)pyridine*

■ INTRODUCTION

The spin-crossover (SCO) or spin transition phenomenon exhibits the interchange of two spin states from the paramagnetic high-spin (HS) to the diamagnetic low-spin (LS) and *vice versa* under the external stimulation effect of temperature changes [1], pressure [2], and irradiation of light [3]. Cambi and coworkers discovered the first SCO phenomenon in a Fe(III) dithiocarbamate mononuclear complex in 1931 [4]. Since then, many SCO materials containing the metal ions of $3d^n$ with n = 4–7 have been synthesized and extensively investigated [5].

Materials exhibiting the SCO phenomenon continue to be intensively studied because of the numerous potential applications for information storage [6], sensors [7], molecular switches [8], etc. Among the SCO materials, many research groups have widely investigated

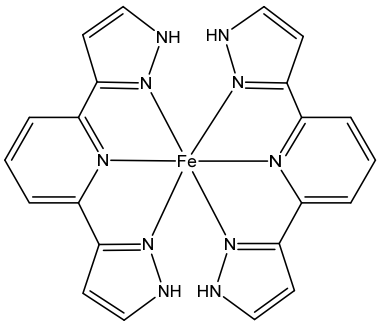

Fig 1. The mononuclear complex of $[Fe(3\text{-}bpp)_2]^{2+}$

the mononuclear complex of $[Fe(3\text{-}bpp)_2]^{2+}$ (Fig. 1) formed by the tridentate of 3-bpp ligand [9]. These complexes are particularly interesting because they can be modified by various counter anions where the difference of counter anions determines the type of spin transition and transition temperature ($T_{1/2}$). Quite recently, the presence of Fe(II) complex in the HS and LS states has been demonstrated by a single crystal of $[Fe(3\text{-}bpp)_2](CF_3COO)_2$ complex in the SCO system [10]. There are several types of spin transition commonly observed in SCO materials such as: gradual, abrupt, hysteretic, stepwise, and incomplete [11], where the $T_{1/2}$ is described as transition temperature which reveals the ratio of HS and LS states in the compound is 50:50.

The spin transition and the transition temperature in SCO materials are affected by the coordination number of metal ions and the nature of ligands and the counter anions type or even solvent molecules [12]. In the complex of $[Fe(3\text{-}bpp)_2]^{2+}$, the 3-bpp ligand is one of the intermediate ligands with the pyrazolyl ring with one nitrogen linked to an H atom free to form hydrogen bonds with the anions. While many oxides and halogenate anions have been investigated, complex anions containing transition metal ions have also been reported in many Fe(II) SCO systems. For example, the $[Fe(3\text{-}bpp)_2][Fe(CN)_5(NO)]$ complex has been synthesized from $[Fe(3\text{-}bpp)_2]^{2+}$ complex with nitroprusside $[Fe(CN)5(NO)]^{2+}$ anion containing Fe(III) metal ion. The complex showed abrupt transition, and the transition temperature occurred below room temperature with small hysteresis ($T_{1/2}\downarrow$ = 181 K; $T_{1/2}\uparrow$ = 184 K) [13]. Moreover, the complex of $[Fe(3\text{-}bpp)_2]^{2+}$ is also conducted using complex cyanide anion $[Au(CN)_2]^-$ containing Au(I) metal ion. The complex of $[Fe(3\text{-}bpp)_2][Au(CN)_2]_2{\cdot}2H_2O$ showed incomplete and very gradual transitions without hysteresis where the $T_{1/2}$ value of the complex can be estimated at 291 K [14]. Meanwhile, the $[Fe(3\text{-}bpp)_2][Au(CN)_2]_2$ complex showed two steps of thermal hysteresis, and the abrupt transition occurred above room temperature, showing $T_{1/2}\downarrow$ = 370 K and $T_{1/2}\uparrow$ = 415 K for the large hysteresis, while the $T_{1/2}\downarrow$ = 420 K and $T_{1/2}\uparrow$ = 430 K for the small one [15]. In this case, the difference in SCO properties from those complexes may be affected by the absence or existence of solvent molecules in the structure of the complex. The existence of solvent molecules in the complex is due to the interaction of hydrogen bonds between the hydrogen atom in the 3-bpp ligand and the oxygen atom in water molecules, with a high electronegative atom. In general, the solvent should be avoided to ensure the short contacts between the 3-bpp ligand and the anions to enhance more cooperative transitions.

The use of metal cyanide complexes as a counter anion, $[M(CN)_2]^-$ with M is Ag or Au, has been reported in the $[Fe(3\text{-}bpp)_2]^{2+}$ complex with various SCO properties [14]. Therefore, in the present study, we describe here the synthesis of $[Fe(3\text{-}bpp)_2][M(CN)_4]$ complex. Since the nitrogen atom of the cyanide (CN^-) ligand has the potential to form hydrogen bonds with a hydrogen atom of the 3-bpp ligand, the strategy synthesis of the complex needs to be elaborated. In addition to that, it is also necessary to study the magnetic property of this complex as an SCO material. In this study, the resulting complex of $[Fe(3\text{-}bpp)_2][Ni(CN)_4]{\cdot}4H_2O$ was characterized by the CHN elemental analysis, thermogravimetric analysis, and AAS measurement to determine its chemical formula. The data of SEM–EDX was evaluated to identify the surface morphology and the composition of elements in the complex. Meanwhile, coordination bonds in the complex were also analyzed from the infrared spectra. The SCO property was studied by measuring the magnetic susceptibility at various temperatures.

■ EXPERIMENTAL SECTION

Materials

The main chemicals of 2,6-(diacethyl)pyridine ($C_9H_9NO_2$), *N*,*N*-dimethylformamide dimethylacetal ($C_5H_{13}NO_2$), hydrazine hydrate (N_2H_4), activated charcoal, iron(II) sulfate heptahydrate ($Fe(SO_4)_2{\cdot}7H_2O$), barium chloride dihydrate ($BaCl_2{\cdot}2H_2O$), and potassium tetracyano nickelate(II) ($K_2[Ni(CN)_4]$). The solvents consist of *n*-hexane (C_6H_{14}), chloroform ($CHCl_3$), ethanol (C_2H_5OH), and methanol (CH_3OH). All chemicals and solvents were used with no further purifications, and they were respectively purchased from Sigma Aldrich and Merck.

Instrumentation

The CHN elemental analysis was measured using the ThermoFisher Scientific FlashSmart CHNS Elemental Analyzer. The metal content of the complex was estimated based on the data recorded using an Atomic Absorption Spectrophotometer (AAS) model of GBC Avanta V2. Thermal decomposition of the $[Fe(3\text{-}bpp)_2][Ni(CN)_4]{\cdot}4H_2O$ complex was performed up to 600 °C under nitrogen and used to confirm the amount of hydrate and the decomposition products of the complex. This analysis was obtained using TG/DTA Hitachi STA7300 thermal analyzer model with a heating rate of 10 °C/min. The infrared spectra of the ligand and the complex were collected using KBr pellets on a ThermoFisher Scientific Model of Nicolet IS5 in the range of 4000–400 cm^{-1}. The SEM image of the complex was recorded in SEM-EDX (Scanning Electron Microscopy with Energy Dispersive X-ray) JEOL JSM 6510 LA model to confirm the mass percentages and the content of the main elements in the sample. The temperature variation from magnetic susceptibility measurement was conducted using a Quantum Design MPMS-XL7A SQUID (Superconducting Quantum Interference Device) magnetometer in the temperature range of 2–300 K under an external 5000 Oe magnetic field.

Procedure

The synthesis procedures of 3-bpp ligand and $[Fe(3\text{-}bpp)_2][Ni(CN)_4]{\cdot}4H_2O$ complex

The 3-bpp ligand or 2,6-bis(pyrazol-3-yl)pyridine was prepared according to the previously published method by Lin and Lang [16]. A mixture containing 2,6-diacetylpyridine (5 g, 30.64 mmol) and *N*,*N*'-dimethylformamide dimethyl acetal (10 mL, 75.28 mmol) was refluxed under an atmosphere of nitrogen for 3–4 h. The reaction mixture was cooled and removed until an orange precipitate formed. Then it was dissolved in chloroform, and the solution was treated with activated charcoal, filtered off, and then concentrated. The yellow precipitate as starting material was crystallized on dilution with *n*-hexane. A suspension of the appropriate starting material (2.5 g) in ethanol (12.5 mL) and hydrazine hydrate (2.5 mL) was stirred for 3–4 h at room temperature. Dilution of the saturated solution with water until a white precipitate formed (3-bpp ligand). Then it was filtered, and the synthesis product was dried in a desiccator over silica gel. The yield was 48–50%. (m.p. 258–260 °C, literature 257–259 °C).

Meanwhile, the $[Fe(3\text{-}bpp)_2][Ni(CN)_4]{\cdot}4H_2O$ complex was synthesized using the following procedure. In 3 mL H_2O containing $FeSO_4{\cdot}7H_2O$ (0.28 g; 1 mmol) with a little addition of ascorbic acid to prevent oxidation of the Fe(II) ion, it was added in 2 mL H_2O solution of $BaCl_2{\cdot}2H_2O$ (0.27 g; 1.1 mmol). The reaction mixture was stirred in a centrifuge for about 45 min. A clear solution containing $FeCl_2$ was separated from the white precipitate of $BaSO_4$ with a syringe. The $FeCl_2$ solution was added dropwise to the solution of 3-bpp ligand (0.5 g; 2.4 mmol) in 30 mL methanol. While the mixture was stirred under an atmosphere of nitrogen, the saturated aqueous solution of $K_2[Ni(CN)_4]$ in excess (4.2 mmol, 3 mL) was then added to the mixture. The red-brown precipitate formed upon the addition. After the reaction mixture was vigorously stirred for about 1–2 h, it was filtered and washed with a small amount of water. The synthesis product was dried over silica gel in a desiccator (Yield: 58–60% w/w).

■ RESULTS AND DISCUSSION

Synthesis and Characterization of $[Fe(3\text{-}bpp)_2][Ni(CN)_4]{\cdot}4H_2O$

The preparation of $[Fe(3\text{-}bpp)_2][Ni(CN)_4]{\cdot}4H_2O$ complex was adopted by a modification of the literature

procedure [11] using the reaction of $FeSO_4$ with $BaCl_2$ in an aqueous solution produced the white precipitate of $BaSO_4$ and a clear solution of $FeCl_2$. Then the $FeCl_2$ solution was added dropwise to the methanolic solution of 3-bpp ligand, resulting in a mixture of red-brown color solution. The red-brown precipitate was formed when an excess of $K_2[Ni(CN)_4]$ salt was added to the mixture solution. Based on the solubility test, the product of red-brown powder was hardly soluble in various commonly known solvents such as water, methanol, ethanol, chloroform, acetone, acetonitrile, and diethyl ether. Therefore, attempts to produce the single crystal of the expected $[Fe(3\text{-bpp})_2][Ni(CN)_4]\cdot 4H_2O$ complex could not be attained.

Table 1 shows the result of CHN elemental analysis and AAS measurement on the elemental composition contained in the synthesized complex. The chemical formula of the complex obtained from the analysis results is $[Fe(C_{11}H_9N_5)_2][Ni(CN)_4]\cdot 4H_2O$, in agreement with the expected chemical formula.

Infrared spectra of [Fe(3-bpp)2][Ni(CN)4]·4H2O complex and 3-bpp ligand recorded at 291 K are shown in Fig. 2. The typical vibration of 3-bpp ligands such as $\nu_{(N\text{-}H)}$ stretching, $\nu_{(C=C)}$ stretching, $\nu_{(C=C\text{-}N)}$ stretching of pyridine, $\nu_{(N\text{-}H)}$ bending, and $\nu_{(C\text{-}H)}$ stretching bands were observed at around 3202, 1595, 1565, 1471, and 806 cm^{-1}, respectively, as previously reported by Gamez et al. [17]. In the infrared spectrum of the $[Fe(3\text{-bpp})_2][Ni(CN)_4]\cdot 4H_2O$ complex, the $\nu_{(C=C\text{-}N)}$ band appeared at 1575 cm^{-1}, which was higher than in the infrared spectrum of 3-bpp ligand (1565 cm^{-1}). The shift of the $\nu_{(C=C\text{-}N)}$ band indicated that the Fe(II) ion is coordinated with the nitrogen atom of the pyridine ring of the 3-bpp ligand. Moreover, the spectrum of the complex exhibited a broad and a medium intense new band at 3435 cm^{-1} due to $\nu_{(OH)}$ of water molecules [18]. The presence of H_2O molecules as a hydrate in the spectrum of the complex was also confirmed by thermogravimetric analysis. Meanwhile, the $\nu_{(C\equiv N)}$ stretching vibration band belonging to the tetracyanonickelate group in the complex was observed at 2131 cm^{-1}. This vibration band usually appears in the 2000–2200 cm^{-1} range with a sharp and strong band. Thus it can be easily identified in the vibration spectrum of

Table 1. The composition of C, H, N, and Fe

Complex	%			
	C	H	N	Fe
Found	43.65	3.39	26.95	7.76
Calculated	43.76	3.65	27.49	7.85

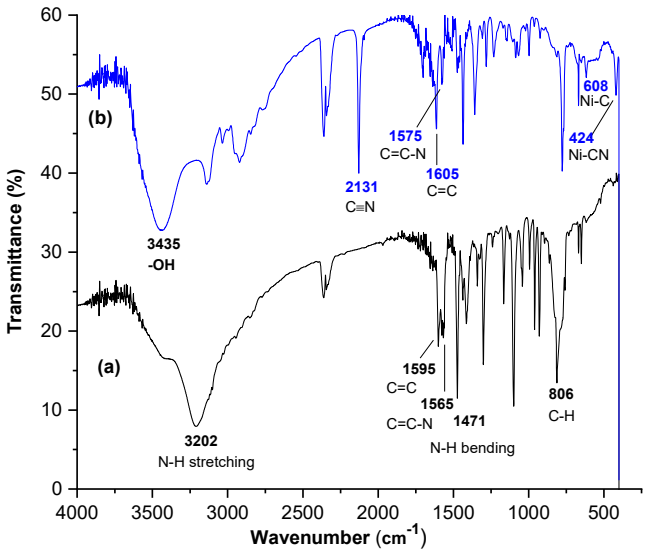

Fig 2. Infrared spectra of (a) 3-bpp ligand and (b) $[Fe(3\text{-bpp})_2][Ni(CN)_4]\cdot 4H_2O$ complex at 291 K

the complex [19]. In addition, the vibration bands of the tetracyanonickelate group in the complexes exhibit M–C stretching and M–C–N bending bands in the range of 400–600 cm^{-1} [20]. These bands were observed at 608 and 424 cm^{-1} in the complex spectrum and might be assigned to the stretching of Ni–C and bending of Ni–CN vibration bands, respectively.

Thermogravimetry analysis of the $[Fe(3\text{-bpp})_2][Ni(CN)_4]\cdot 4H_2O$ complex was performed to confirm the number of hydrates of the chemical formula and decomposition of the complex as well as the temperature range of the stability of the complex. As shown in Fig. 3, the thermal decomposition in the first and the second steps are due to the dehydration process of the complex. The thermogram displays weight losses at around 8.07 and 2.71% in the temperature range of 30–85 °C and 85–135 °C, respectively, corresponding to the total decomposition of four uncoordinated water molecules (calculated as 10.10%, found 10.78%). These results show a good agreement with the composition determined from the elemental analysis data. The loss of

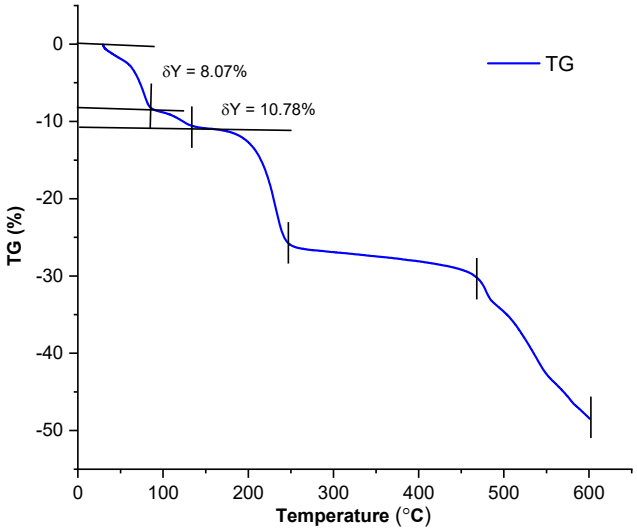

Fig 3. Thermogravimetry (TG) profile of $[Fe(3\text{-}bpp)_2][Ni(CN)_4]\cdot 4H_2O$ complex

uncoordinated water molecules usually occurs below 200 °C. As reported previously, the $[Fe(3\text{-}bpp)_2](C_6H_4NO_2)_2\cdot 4H_2O$ complex started to decompose with three water molecules and one water molecule at 54 °C and 170–220 °C temperature range, respectively [21]. While the next weight loss of about 14.26% (calculated as 14.59%) in the temperature range of 135–240 °C could be attributed to the loss of CN groups. Cordoba et al. [22] suggested that the loss of CN groups in the $SrNH_4[Fe(CN)_6]\cdot 3H_2O$ compound occurred at 150–290 °C. The continuous weight loss appears in the temperature range of 240–470 °C and 470–600 °C, which could be associated with the loss of 3-bpp ligand and the residue of the complex, respectively. The final decomposition product could be identified as FeO and NiO (calculated as 20.62%, found at 19.88%) within 470–600 °C. Thermal decomposition products have also been observed by Karaağaç and Kürkçüoğlu [23] in the cyano metal complexes with the loss of metal oxides (CuO, ZnO, and NiO) appearing by the thermogram below 700 °C.

The surface morphology and elemental content in the $[Fe(3\text{-}bpp)_2][Ni(CN)_4]\cdot 4H_2O$ complex were also determined by SEM–EDX. The selected surface of the SEM image of the complex exhibits cubic shapes on the scale of 20 μm, as depicted in Fig. 4(a). Meanwhile, the existence of the corresponding elemental content in the complex, except the hydrogen atom, was displayed in Fig. 4(b). This study used the EDX analysis to determine the mass percentages of Fe and Ni in the state of a complex compound (Table 2). Based on the EDX analysis result, the obtained Fe and Ni mass percentages were respectively 6.29 and 8.61%. These percentages were almost equal to the calculated Fe and Ni mass percentages

Table 2. The mass percentage of Fe and Ni atoms in the $[Fe(3\text{-}bpp)_2][Ni(CN)_4]\cdot 4H_2O$ complex

Atom	% Mass
C	47.80
N	36.67
O	0.63
Fe	6.29
Ni	8.61

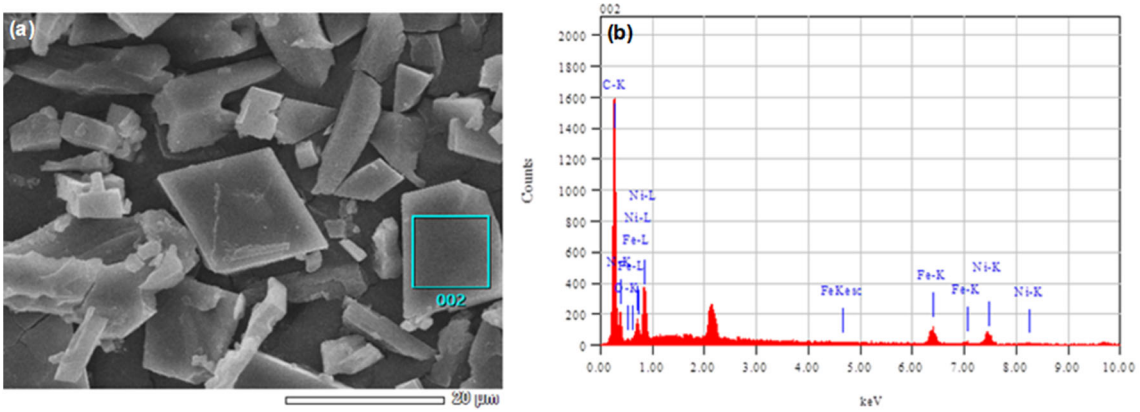

Fig 4. The image of (a) the selected surface of $[Fe(3\text{-}bpp)_2][Ni(CN)_4]\cdot 4H_2O$ complex and its (b) EDX analysis result showing the content of elements, Fe-C-N-O-Ni

of 7.85 and 8.27%, respectively. The results indicate a good agreement with the amount of Fe in the metal content (AAS). The result was 7.76%, which concluded that the chemical formula of the complex being $[Fe(3\text{-}bpp)_2][Ni(CN)_4]\cdot 4H_2O$.

Magnetic Susceptibility

Magnetic susceptibility data of $[Fe(3\text{-}bpp)_2][Ni(CN)_4]\cdot 4H_2O$ complex was collected in the temperature range of 2–300 K at cooling and heating modes. Fig. 5 displays the temperature dependence of the X_MT for $[Fe(3\text{-}bpp)_2][Ni(CN)_4]\cdot 4H_2O$ complex with the molar magnetic susceptibility is X_M, and the temperature is T. At first, the X_MT was measured from 300 K down to 2 K. After the cooling process, the X_MT was measured from 2 K up to 300 K within the heating process. At 300 K, the X_MT value is 2.65 emu mol^{-1} K, suggesting that about 75% of Fe(II) complex is in the HS state at this temperature since the HS of $[Fe(3\text{-}bpp)2]^{2+}$ shows the X_MT value is 3.5 ± 0.1 emu mol^{-1} K [24-25]. On decreasing the temperature from 300 K, the X_MT value of the complex gradually decreases around 1.37 emu mol^{-1} K at 13 K. Below 13 K. The X_MT value was abruptly decreased due to weak anti-ferromagnetic exchange interactions between the Fe^{2+} ion and/or by the zero-field splitting (ZFS) effect associated with the Fe^{2+} ion in the HS state. The final X_MT value reaches about 0.73 emu mol^{-1} K at 2 K, indicative of the complex being in the LS state. Compared to the previously described by King et al. [14], the $[Fe(3\text{-}bpp)_2][Au(CN)_2]_2\cdot 2H_2O$ complex showed a very gradual transition, and the partial conversion was incomplete. The X_MT value of the complex was 1.9 emu mol^{-1} K at 300 K, implying that the Fe(II) complex was 55–60% HS state at room temperature. On cooling, the X_MT value of the complex decreased to 0.6 emu mol^{-1} K at 150 K. The $T_{1/2}$ value can be estimated at 291 K, where the complex's HS and LS fractions equal 50%.

In this study, the plot of high-spin fraction (γ_{HS}) versus temperature in Fig. 5(b) for the $[Fe(3\text{-}bpp)_2][Ni(CN)_4]\cdot 4H_2O$ complex was measured during cooling and heating modes with the estimated of transition temperature ($T_{1/2}$) is halfway, $\gamma_{HS} = \gamma_{LS} = 0.5$. Therefore, this complex shows a gradual spin transition with an estimated $T_{1/2}$ value close to 140 K at $\gamma_{HS} = 0.5$ and no evidence of hysteretic behavior upon cooling and heating modes. Based on the result, the difference in transition temperature occurred from the $[Fe(3\text{-}bpp)_2]^{2+}$ complex cation with different metal cyanide anions, as previously described. Even with the same ligand, the nature of metal cyanide anions with varying amounts of oxidation and solvent molecules in the complexes significantly affects the spin transition and the transition temperature based on the magnetic data.

In addition, the change in magnetism due to the temperature change is supported by an apparent and reversible color change from red-brown at room temperature to dark brown on cooling in liquid nitrogen.

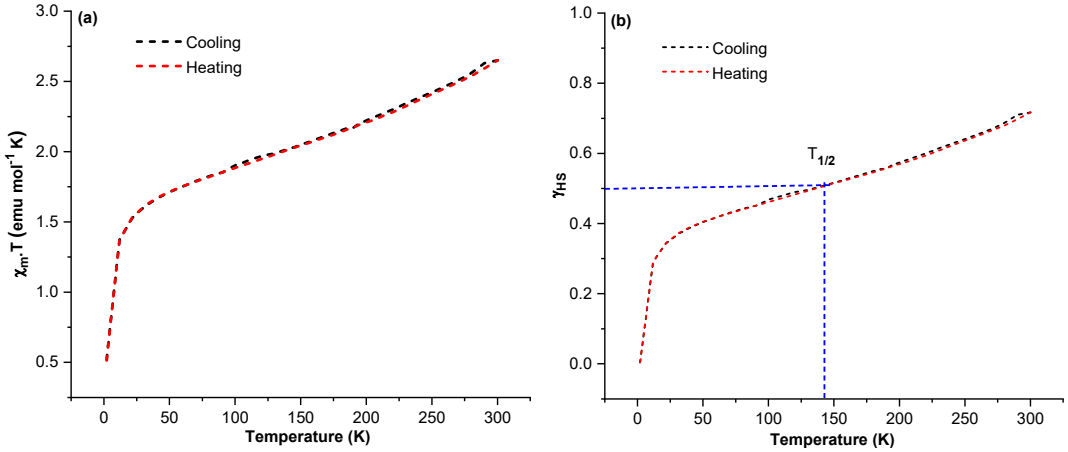

Fig 5. Magnetic susceptibility of (a) $[Fe(3\text{-}bpp)_2][Ni(CN)_4]\cdot 4H_2O$ complex and (b) its variation of high-spin fraction (γ_{HS}) with temperature during cooling and heating modes

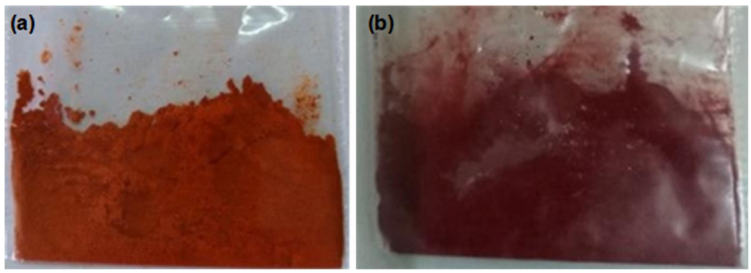

Fig 6. Color of $[Fe(3\text{-}bpp)_2][Ni(CN)_4]\cdot 4H_2O$ complex (a) at 298 K and (b) in liquid nitrogen

Thus, the thermochromic nature of the $[Fe(3\text{-}bpp)_2][Ni(CN)_4]\cdot 4H_2O$ complex suggests the occurrence of spin crossover property, as shown in Fig. 6.

■ CONCLUSION

The complex containing $[Fe(3\text{-}bpp)_2]^{2+}$ cation and $[Ni(CN)_4]^{2-}$ anion has been successfully synthesized and characterized. The chemical formula of $[Fe(3\text{-}bpp)_2][Ni(CN)_4]\cdot 4H_2O$ complex was estimated by AAS, while the existence of water molecules in the complex was also determined using thermal analysis. The presence of elemental content in the complex, except for the hydrogen atom, was confirmed by SEM–EDX analysis. The infrared spectra show the typical vibration bands of functional groups for the 3-bpp ligand as well as the $[Ni(CN)4]^{2-}$ anion. Moreover, the temperature dependence of the complex finds that the X_MT value at 300 K is 2.65 emu mol^{-1} K, where about 75% of the Fe(II) complex is in the HS state. Upon cooling, the X_MT value gradually decreases around 1.37 emu mol^{-1} K at 13 K. Then it decreases abruptly on cooling down to 2 K, where the X_MT value is 0.73 emu mol^{-1} K, indicating that Fe(II) complex is almost entirely in the LS state. The gradual spin transition has a $T_{1/2}$ value close to 140 K, and hysteretic behavior was not observed at cooling and heating modes. The SCO property of this complex was also supported by a reversible change of color from red-brown (HS) to dark brown (LS).

■ ACKNOWLEDGMENTS

The authors thank the World Class Research (WRC) Grant under contract No. 122L/IT1.C02/TA.00/2021 and 5D/IT1.C02/TA.002022. Fitriani is grateful to the LPDP Kementerian Keuangan RI (Indonesia Endowment Fund for Education Ministry of Finance Republic Indonesia) for financial support and Doctoral scholarship.

■ AUTHOR CONTRIBUTIONS

Fitriani, Djulia Onggo, and Irma Mulyani conducted the synthesis of complex and TG/DTA analysis; Kristian Handoyo Sugiyarto, Ashis Bhattacharjee, Hiroki Akutsu, and Anas Santria conducted the magnetic susceptibility analysis; Fitriani, Djulia Onggo, Irma Mulyani, Kristian Handoyo Sugiyarto, Ashis Bhattacharjee, Hiroki Akutsu, and Anas Santria wrote and corrected the manuscript. All authors approved the final version of this manuscript.

■ REFERENCES

[1] Brooker, S., 2015, Spin crossover with thermal hysteresis: Practicalities and lessons learnt, *Chem. Soc. Rev.*, 44 (10), 2880–2892.

[2] Gaspar, A.B., Molnár, G., Rotaru, A., and Shepherd, H.J., 2018, Pressure effect investigations on spin-crossover coordination compounds, *C.R. Chim.*, 21 (12), 1095–1120.

[3] Chastanet, G., Desplanches, C., Baldé, C., Rosa, P., Marchivie, M., and Guionneau, P., 2018, A critical review of the T(LIESST) temperature in spin crossover materials – What it is and what it is not, *Chem. Sq.*, 2, 21–18.

[4] Cambi, L., and Szego, L., 1931, Uber die magnetische susceptibilitat der komplexen verbindungen, *Ber. Dtsch. Chem. Ges. B*, 64 (10), 2591–2598.

[5] Gütlich, P., Gaspar, A.B., and Garcia, Y., 2013, Spin state switching in iron coordination compound, *Beilstein J. Org. Chem.*, 9, 342–391.

[6] Kumar, K.S., and Ruben, M., 2017, Emerging trends in spin crossover (SCO) based functional materials and devices, *Coord. Chem. Rev.*, 346, 176–205.

[7] Jureschi, C.M., Linares, J., Boulmaali, A., Dahoo, P.R., Rotaru, A., and Garcia, Y., 2016, Pressure and temperature sensors using two spin crossover materials, *Sensors*, 16 (2), 187.

[8] Hayami, S., Holmes, S.M., and Halcrow, M.A., 2015, Spin-state switches in molecular materials chemistry, *J. Mater. Chem. C*, 3 (30), 7775–7778.

[9] Halcrow, M.A., 2014, Recent advances in the synthesis and applications of 2,6-dipyrazolylpyridine derivatives and their complexes, *New J. Chem.*, 38 (5), 1868–1882.

[10] Sugiyarto, K.H., Onggo, D., Akutsu, H., Reddy, V.R., Sutrisno, H., Nakazawa, Y., and Bhattacharjee, A., 2021, Structural, magnetic and Mössbauer spectroscopic studies of the $[Fe(3\text{-}bpp)_2](CF_3COO)_2$ complex: role of crystal packing leading to an incomplete Fe(II) high spin ⇋ low spin transition, *CrystEngComm*, 23 (15), 2854–2861.

[11] Gutlich, P., and Goodwin, H.A., 2014, Spin crossover an overall perspective, *Top. Curr. Chem.*, 233, 1–47.

[12] Milin, E., Benaicha, B., El Hajj, F., Patinec, V., Triki, S., Marchivie, M., Gomez-Garcia, C.J., and Pillet, S., 2016, Magnetic bistability in macrocycle-based Fe(II) spin-crossover complexes: Counter ion and solvent effects, *Eur. J. Inorg. Chem.*, 2016 (34), 5305–5314.

[13] Sugiyarto, K.H., McHale, W.A., Craig, D.C., Rae, A.D., Scudder, M.L., and Goodwin, H.A., 2003, Spin transition centres linked by the nitroprusside ion. The cooperative transition in bis(2,6-bis(pyrazol-3-yl)-pyridine)iron(II) nitroprusside, *Dalton Trans.*, 12, 2443–2448.

[14] King, P., Henkelis, J.J., Kilner, C.A., and Halcrow, M.A., 2013, Four new spin-crossover salts of $[Fe(3\text{-}bpp)_2]^{2+}$ (3-bpp=2,6-bis[1H-pyrazol-3-yl]pyridine), *Polyhedron*, 52, 1449–1456.

[15] Djemel, A., Stefanczyk, O., Marchivie, M., Trzop, E., Collet, E., Desplanches, C., Delimi, R., and Chastanet, G., 2018, Solvatomorphism-induced 45 K hysteresis width in a spin crossover mononuclear compound, *Chem. - Eur. J.*, 24 (55), 14760–14767.

[16] Lin, Y., and Lang, S.A., 1977, Novel two step synthesis of pyrazoles and isoxazoles from aryl methyl ketones, *J. Heterocycl. Chem.*, 14 (2), 345–347.

[17] Gamez, P., Steensma, R.H., Driessen, W.L., and Reedijk, J., 2002, Copper(II) compounds of the planar-tridentate ligand 2,6-bis(pyrazol-3-yl)pyridine, *Inorg. Chim. Acta*, 333 (1), 51–56.

[18] Tobon, Y.A., Kabalan, L., Bonhommeau, S., Daro, N., Grosjean, A., Guionneau, P., Matar, S., Létard, J.F., and Guillaume, F., 2013, Spin crossover complexes $[Fe(NH_2trz)_3](X)_2{\cdot}nH_2O$ investigated by means of Raman scattering and DFT calculations, *Phys. Chem. Chem. Phys.*, 15 (41), 18128–18137.

[19] Karaağaç, D., and Kürkçüoğlu, G.S., 2015, Syntheses, spectroscopic and thermal analyses of the Hofmann-type metal(II) tetracyanonickelate(II) pyridazine complexes: $\{[M(pdz)Ni(CN)_4]\cdot H_2O\}n$ (M = Zn(II) or Cd(II)), *Bull. Chem. Soc. Ethiop.*, 29 (3), 415–422.

[20] Karaağaç, D., and Kürkçüoglu, G.S., 2015, Syntheses, spectroscopic and thermal analyses of cyanide bridged heteronuclear polymeric complexes: $[M(L)_2Ni(CN)_4]_n$(L=*N*-methylethylenediamine or *N*-ethylethylenediamine; M]Ni(II), Cu(II), Zn(II) or Cd(II)), *J. Mol. Struct.*, 1105, 263–272.

[21] Jornet-Mollá, V., Giménez-Saiz, C., and Romero, F.M., 2018, synthesis, structure, and photomagnetic properties of a hydrogen-bonded lattice of $[Fe(bpp)_2]^{2+}$ spin-crossover complexes and nicotinate anions, *Crystals*, 8 (11), 439.

[22] Córdoba, L.M., Gómez, M.I., Morán, J.A., and Aymonino, P.J., 2008, Synthesis of the $SrFeO_{2.5}$ and $BaFeO_{3\text{-}x}$ perovskites by thermal decomposition of $SrNH_4[Fe(CN)_6]3H_2O$ and $BaNH_4[Fe(CN)_6]$, *J. Argent. Chem. Soc.*, 96 (1-2), 1–12.

[23] Karaağaç, D., and Kürkçüoğlu, G.S., 2016, Syntheses and characterizations of the cyanide-bridged heteronuclear polymeric complexes with 2-ethylimidazole, *Bull. Chem. Soc. Ethiop.*, 30 (2), 263–272.

[24] Roberts, T.D., Little, M.A., Cook, L.J.K., and Halcrow, M.A., 2014, Iron(II) complexes of 2,6-

di(1*H*-pyrazol-3-yl)-pyridine derivatives with hydrogen bonding and sterically bulky substituents, *Dalton Trans.*, 43 (20), 7577–7588.

[25] Djemel, A., Stefanczyk, O., Desplanches, C., Kumar, K., Delimi, R., Benaceur, F., Ohkoshi, S.I., and Chastanet, G., 2021, Switching on thermal and light-induced spin crossover by desolvation of $[Fe(3\text{-bpp})_2](XO_4)_2$·solvent (X = Cl, Re) compounds, *Inorg. Chem. Front.*, 8 (13), 3210–3221.